

12

6

WAVE PROPAGATION, ELASTODYNAMIC STRESS
SINGULARITIES AND FRACTURE .

9

Interim rept.

by

10

J. D. Achenbach

Department of Civil Engineering
The Technological Institute
Northwestern University
Evanston, Illinois 60201

11

May 76

12

19p.

15

Office of Naval Research

~~NOO~~14-76-C-0063

✓ NSF-ENG-70-01465

May 1976

14

NU-SML-TR ~~NO~~-76-1

9

DDC
RECEIVED
SEP 14 1976
B

Approved for public release; distribution unlimited

16

NR-064-483

ADA 029665

1473
400444
LB

WAVE PROPAGATION, ELASTODYNAMIC STRESS SINGULARITIES, AND FRACTURE

J. D. Achenbach

Department of Civil Engineering
Northwestern University
Evanston, Illinois 60201
USA

The singular part of the elastodynamic field in the vicinity of a crack tip plays an important role in fracture mechanics considerations. In this paper analytical, numerical and experimental methods to determine near-tip elastodynamic fields are reviewed, and the interpretation of stress intensity factors is discussed within the context of the fracture criterion of the balance of rates of energies. We consider elastodynamic effects generated by rapid propagation of the crack as well as by the diffraction of incident stress waves. Propagation in the plane of the crack, as well as skew crack propagation and crack bifurcation are investigated. Necessary conditions for these kinds of crack propagation are discussed, and expressions are derived for crack tip speeds.

1. INTRODUCTION

The singular behavior at edges and corners of solutions to the system of partial differential equations governing linearized elasticity has fascinated many mathematically inclined investigators. From the analytical point of view this pathological behavior of the field quantities must be unraveled, if for no other reason than one which impels mountain climbers to climb: the singularities are there! From the physical point of view there is the additional challenge of trying to come to grips with singular stresses and strains within the framework of a physical theory. Attempts to respond to that challenge are, however, bound to generate controversy. Indeed, singularities are disturbing not only because no real material can actually sustain singular stresses and strains, but also because the basic premises of the linearized theory are violated by the appearance of singularities. To one school of thought the analysis of singularities is, therefore, a futile exercise. What should be done, the protagonists of that view say, is to take into account nonlinear plastic deformation near a sharp edge. Unfortunately this is easier said than done, especially for dynamic problems. It would require much detailed information on the geometry and the material behavior near the edge, and a considerable amount of computer analysis. It is, therefore, a legitimate question whether the easily obtained results of linearized theory can serve a useful purpose, on the basis of an appropriate interpretation of singularities. The conspicuous success of linearized elastic fracture mechanics in placing square root singularities, which occur at crack tips, in the framework of a useful fracture criterion, is heartening to those who have spent some of their efforts on analyzing fields near crack tips on the basis of linear elastodynamic theory.

The title of this survey paper may suggest a more ambitious enterprise than is intended. Each of the topics wave propagation, elastodynamic stress singularities, and fracture,

represents a broad spectrum of research activity, each worthy of an attempt to survey recent contributions and identify significant unsolved problems. The objective of this paper is, however, rather more limited in scope, in that it is directed towards an account of recent developments in a relatively small area, comprising the region of overlap of the sprawling domains of the topics stated in the title.

The topic of wave propagation needs only a few words of introduction. Local excitation of a body is not instantaneously detected at positions that are at a distance from the region of excitation. It takes time, albeit a very short time, for a disturbance to propagate from its source to other positions. As elements of the medium are deformed the disturbance is transmitted from one point to the next and the disturbance, or wave, progresses through the solid. In this process the resistance offered to deformation by the consistency of the solid, as well as the resistance to motion offered by inertia must be overcome.

During the last three or four years a number of books have been published dealing with the propagation of waves in elastic solids. Among these, the books by Achenbach [1], Pao and Mow [2], and Eringen and Suhubi [3], are most directly relevant to the material of this paper.

In the analysis of dynamic problems it is often found that at inhomogeneities in a body the dynamic stresses are higher than the stresses computed from the corresponding problem of static equilibrium. This occurs when a propagating mechanical disturbance strikes a cavity, see e.g. Ref. [2] for specific examples. The dynamic stress "overshoot" is especially pronounced if the cavity contains a sharp edge. For a crack the intensity of the stress field in the vicinity of the crack tip can be very significantly affected by dynamic effects, as will be discussed in more detail later in this paper. In view of the dynamic amplification, it is conceivable that there are cases for which fracture at a

crack tip does not occur under a gradually applied system of loads, but where a crack does indeed propagate when the same system of loads is rapidly applied, and gives rise to waves (as for impact loads and explosive charges). Dynamic effects on the fields near a crack tip become also significant if the propagation of the crack is very fast, so that rapid motions are generated in the solid. Earthquakes are an example of significant dynamic effects generated by a fracture phenomenon. Essentially brittle fracture in engineering materials, and in glass, which is often of an explosive nature, provides other examples. In Reference [4] a number of observations on the influence of elastodynamic effects are presented on the basis of solutions of example problems. An extensive list of references is included in Ref. [4]. A recent article by Freund [5] also discusses in detail the analysis of elastodynamic crack tip stress fields.

In this paper we review some old results, and we present some new ones on the dynamic stress field in the vicinity of a crack tip. We consider elastodynamic effects generated by rapid crack propagation, as well as by the diffraction of incident stress waves. In both cases the crack tip is in an environment disturbed by elastic wave motions. Propagation in the plane of the crack as well as skew crack propagation and crack bifurcation are investigated. The emphasis is on the computation of elastodynamic singularities, and the interpretation of the strengths of these singularities within the context of the fracture criterion of the balance of rates of energies.

The results discussed in this paper are obtained on the basis of the equations governing linearized elastodynamics for a homogeneous, isotropic solid. Let $u_i(x_m, t)$ be the components of the displacement vector in a rectangular Cartesian coordinate system with coordinates x_i , $i = 1, 2, 3$. The components of the stress tensor, τ_{ij} , are related to the gradients of the displacement vector by Hooke's law:

$$\tau_{ij} = \lambda u_{k,k} \delta_{ij} + \mu (u_{i,j} + u_{j,i}) \quad (1.1)$$

Here $u_{i,j} \equiv \partial u_i(x_m) / \partial x_j$, and repeated indices indicate a summation. Also, λ and μ are Lamé's elastic constants, and δ_{ij} is the Kronecker delta. Substitution of Eq. (1.1) into the stress equations of motion yields

$$\mu u_{i,jj} + (\lambda + \mu) u_{j,ji} = \rho \ddot{u}_i \quad (1.2)$$

In Eq. (1.2) a dot over a quantity denotes a partial derivative with respect to time, and ρ is the mass density.

Equations (1.2) form a somewhat awkward system of coupled partial differential equations. For many elastodynamic problems it is convenient to

express the displacement vector in terms of a scalar potential φ and a vector potential with components ψ_k , by

$$u_i = \varphi_{,i} + e_{ijk} \psi_{k,j} \quad (1.3)$$

with

$$\psi_{k,k} \equiv 0 \quad (1.4)$$

Here e_{ijk} is the alternating symbol of cartesian tensor analysis. It is easy to show by direct substitution that the representation (1.3) satisfies the displacement equation of motion (1.2) if φ and ψ_k are solutions of the wave equations

$$\varphi_{,jj} = \frac{1}{2} \ddot{\varphi}, \quad c_L^2 = \frac{\lambda + 2\mu}{\rho} \quad (1.5a, b)$$

$$\psi_{k,jj} = \frac{1}{2} \ddot{\psi}_k, \quad c_T^2 = \frac{\mu}{\rho} \quad (1.6a, b)$$

Thus, φ and ψ_k satisfy uncoupled wave equations, with wave speeds c_L and c_T , respectively.

When the field variables are independent of one of the Cartesian coordinates, say x_3 , elastic wave motions uncouple into anti-plane and in-plane motions. The displacement $u_3(x_1, x_2, t)$ which describes motions in anti-plane strain, is governed by $u_{3,\alpha\alpha} = (1/c_T^2) \ddot{u}_3$, where $\alpha = 1, 2$. Motions in plane strain are described by displacement components $u_1(x_1, x_2, t)$ and $u_2(x_1, x_2, t)$. For in-plane motions the use of Eq. (1.3) is convenient where there is only one component ψ_k , namely, ψ_3 .

For a detailed presentation of the equations governing linearized elastodynamic theory, we refer to Achenbach[1].

2. ELASTODYNAMIC STRESS INTENSITY FACTORS

The equations governing linearized elasticity were fully developed by the middle of the 19th century. It took another fifty years before the first mathematical analysis of a stress concentration effect based on elastostatic theory was published. In 1898, Kirsch investigated the two-dimensional stress distribution around a small circular hole in a large body subjected to longitudinal tension. He showed that the peak circumferential stress at the hole is three times larger than the unperturbed stress. A few years later stresses near an elliptic hole of semiaxes a, b ($a > b$) were analyzed by Kolosoff and by Inglis. In the limit $b \rightarrow 0$ the latter studies provide results for a crack of width $2a$. The limit process produces a stress field with square root singularities at the crack tips. Numerous results have been published subsequently, for many crack geometries. For a recent review we refer to Ref. [6].

The start of work pertinent to elastodynamic stress singularities can be traced to a classical paper by Sommerfeld, on the diffraction of light by a semi-infinite screen. An account of the approach used can also be found in Sommerfeld's book [7]. For the field variable u satisfying the two-dimensional scalar wave equation, Sommerfeld required that $r \text{ grad } u \rightarrow 0$ as $r \rightarrow 0$. He pointed out that this condition is satisfied when the stationary edge of the screen neither radiates nor absorbs energy. From the mathematical point of view this requirement is an additional energy condition which secures uniqueness of the solution. J. Meixner established the more general condition that the energy density at the edge of the screen should be integrable with respect to space. The edge condition for time harmonic elastodynamic diffraction problems was discussed by Maue [8]. Modifications of the linear elastodynamic uniqueness theorem to extend its range of applicability to include square root singularities near the tip of a running crack were presented by Freund and Clifton [9].

2.1 Stress-Intensity Factors

A crack in a solid body gives rise to a surface of discontinuity of the displacement vector. In general all three components of the displacement vector suffer discontinuities. In a plane two-dimensional geometry in-plane and anti-plane displacements uncouple, and it becomes relatively simple to analyze the fields. It is found that in the neighborhood of the crack tip, the stress components τ_{ij} in a local coordinate system are of the general forms

$$\tau_{ij}(r, \theta, t) = r^{-\frac{1}{2}} F_{ij}(\theta, t) \quad (2.1)$$

Here r and θ are polar coordinates centered at the crack tip. Separate expressions for $F_{ij}(\theta, t)$ are obtained for in-plane displacements that are symmetric and antisymmetric, respectively, with respect to the plane of the crack, and for anti-plane displacements. In the parlance of fracture mechanics the in-plane symmetric and antisymmetric displacements correspond to Mode I and Mode II fracture, respectively. Antiplane displacements correspond to Mode III (tearing) fracture. The function $F_{ij}(\theta, t)$ can be written as

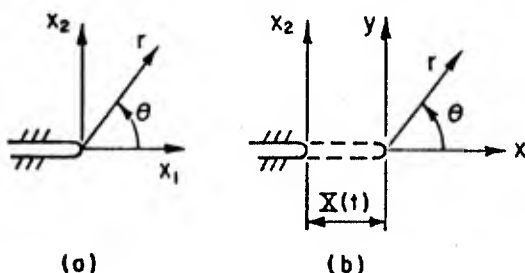


FIGURE 1: Stationary and Propagating crack tips in two-dimensional geometry.

the product of a "stress intensity factor" and a function defining the variation with angle θ . The latter function is universal in that it is independent of the overall geometry and the loading. Overall geometry and loading enter in the stress intensity factor.

In this section we investigate in some detail the near-tip behavior of the stress components τ_{θ} (Mode I) and $\tau_{\theta 3}$ (Mode III), in the polar coordinate systems shown in Fig. 1, for both the elastostatic and the elastodynamic case, and for a stationary as well as a running crack tip.

For the elastostatic case we have

$$\tau_{\theta} = (2\pi)^{-\frac{1}{2}} r^{-\frac{1}{2}} K_I(t) T_{\theta}^I(\theta) \quad (2.2)$$

$$\tau_{\theta 3} = (2\pi)^{-\frac{1}{2}} r^{-\frac{1}{2}} K_{III}(t) T_{\theta 3}^{III}(\theta) \quad (2.3)$$

In these expressions $T_{\theta}^I(0) = T_{\theta 3}^{III}(0) \equiv 1$. For

the elastostatic case the time t is a parameter, which may enter via the loading, or via the length of the crack if the crack is propagating.

The expressions corresponding to Eqs. (2.2) and (2.3) for the elastodynamic case of a stationary crack tip, are completely equivalent in form.

The same angular distributions $T_{\theta}^I(\theta)$ and $T_{\theta 3}^{III}(\theta)$ hold, but the stress intensity factors are of different forms. We use the notation

$$k_I(t) \text{ and } k_{III}(t) \quad (2.4a,b)$$

for the elastodynamic near-tip fields.

The nature of the angular distributions changes for the elastodynamic case of a propagating crack tip. Now the speed of propagation of the crack tip, $v(t)$, enters the expressions for the angular distributions. We use the notations

$$T_{\theta}^I(\theta, v) \text{ and } T_{\theta 3}^{III}(\theta, v) \quad (2.5a,b)$$

where $T_{\theta}^I(0, v) = T_{\theta 3}^{III}(0, v) \equiv 1$. For the stress intensity factors we use the notations

$$k_I(t, v) \text{ and } k_{III}(t, v) \quad (2.6a,b)$$

The expressions of this section also apply to three dimensional problems for a plane crack with a smoothly curved edge. Let a point O on the edge serve as origin for a local Cartesian coordinate system. The x_3 -axis is directed along the tangent to the edge of the crack, the x_2 -axis is normal to the plane of the closed crack, and the x_1 -axis is directed into the solid. In the plane $x_3 = 0$, and in the neighborhood of O , the stress components then are of the forms given by Eqs. (2.1)-(2.6). The geometrical details of the crack edge enter of course in the magnitudes of the stress intensity factors.

2.2 Functions $T_{\theta}^I(\theta)$ and $T_{\theta 3}^{III}(\theta)$

Figure 2 shows a two-dimensional geometry of a wedge-shaped body, which is unbounded in the x_3 -direction. For the two-dimensional case it is simple to analyze the asymptotic behavior of the fields near the vertex of the wedge, by a technique which was employed by Knein, by Williams, and by Karel and Karp [10]. One considers solutions, say for the displacements, of the general separation of variables forms

$$u_r(r, \theta, t) = r^p f(t) U_r(\theta) \quad (2.7)$$

$$u_{\theta}(r, \theta, t) = r^p f(t) U_{\theta}(\theta) \quad (2.8)$$

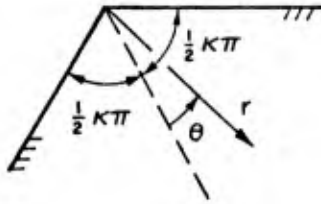


FIGURE 2: Elastic wedge

Substitution into the displacement equations of motion, Eq. (1.2), yields in the limit $r \rightarrow 0$ a coupled system of ordinary differential equations, which contain p as a parameter. Solutions to these equations are

$$U_r(\theta) = A \cos(1+p)\theta + B \sin(1+p)\theta + C \cos(1-p)\theta + D \sin(1-p)\theta \quad (2.9)$$

$$U_{\theta}(\theta) = B \cos(1+p)\theta - A \sin(1+p)\theta + n D \cos(1-p)\theta - n C \sin(1-p)\theta \quad (2.10)$$

where $n = [\mu(1-p) + (\lambda + 2\mu)(1+p)] / [(\lambda + 2\mu)(1-p) + \mu(1+p)]$. The corresponding expressions for the stress components τ_{θ} and $\tau_{r\theta}$ can be computed from Hooke's Law. The dominant terms in the stresses are of the forms

$$\tau_{\theta}, \tau_{r\theta} \sim r^{p-1} \quad (2.11)$$

By invoking the boundary conditions, four equations for the unknown constants, A , B , C and D are obtained. These equations split into two pairs: for displacements which are symmetric and antisymmetric, respectively, relative to $\theta = 0$. The sets of equations possess non-trivial solutions only if the determinants of the coefficients are zero. For symmetric displacements relative to $\theta = 0$ we find

$$B \equiv 0, \quad D \equiv 0 \quad (2.12)$$

$$C = \frac{-2p \sin \frac{1}{2}(1+p)\kappa\pi}{(1-p)(1-n) \sin \frac{1}{2}(1-p)\kappa\pi} A \quad (2.13)$$

$$\frac{\sin(\kappa\pi)}{\kappa\pi} + \frac{\sin(p\kappa\pi)}{p\kappa\pi} = 0 \quad (2.14)$$

The roots of Eq. (2.14) have been studied by Karel and Karp [10]. Naturally one is interested only in those roots for which the strain energy density is integrable in a finite region near the vertex, i.e., roots for which the real parts of p are positive. Only the smallest non-trivial root for each value $\kappa\pi$ need be considered, since the corresponding term dominates the behavior of the stress field in the vicinity of the vertex. When $\kappa\pi < \pi$, the stresses are finite. The smallest value of p occurs at $\kappa = 2$, when $p = 0.5$. This case corresponds to a crack of zero thickness.

For $\kappa = 2$ the near-tip displacements for the symmetric case (Mode I) follow from Eqs. (2.9)-(2.14). The corresponding expression for $T_{\theta}^I(\theta)$ is

$$T_{\theta}^I = \frac{1}{2} (1 + \cos\theta) \cos\left(\frac{1}{2}\theta\right) \quad (2.15)$$

The anti-plane case is still easier to analyze. The result is

$$T_{\theta 3}^{III}(\theta) = \cos\left(\frac{1}{2}\theta\right) \quad (2.16)$$

2.3 Functions $T_{\theta}^I(\theta, v)$ and $T_{\theta 3}^{III}(\theta, v)$

The elastodynamic near-tip field for the case that the tip propagates rapidly along a rather arbitrary but smooth trajectory was discussed by Achenbach and Bažant [11]. Here we consider a crack propagating in its own plane. The two-dimensional geometry is shown in Fig. 1b. The speed of the crack tip is $v(t)$, where $v(t)$ is an arbitrary function of time, subject to the conditions that $v(t)$ and dv/dt are continuous. A system of moving Cartesian coordinates (x, y) is centered at the crack tip, such that the x -axis is in the plane of the crack.

To analyze the in-plane motions it is convenient to express the displacements $u_1(x_1, x_2, t)$ and $u_2(x_1, x_2, t)$ in terms of the displacement potentials ϕ and ψ , see Eq. (1.3). Let the displacement potentials be instantaneously defined in terms of the moving coordinate system (x, y) , i.e., $\phi = \phi(x, y, t)$. The second material derivative with respect to time, which is indicated by a superscript double dot, is then of the form

$$\ddot{\phi} = \frac{\partial^2 \phi}{\partial t^2} - \frac{dv}{dt} \frac{\partial \phi}{\partial x} - 2v(t) \frac{\partial^2 \phi}{\partial t \partial x} + [v(t)]^2 \frac{\partial^2 \phi}{\partial x^2} \quad (2.17)$$

Relative to the moving system of Cartesian coordinates the equation for ϕ is $\nabla^2 \phi = \ddot{\phi}/c_L^2$, where c_L is defined by Eq. (1.5b). A completely analogous equation, with c_T instead of c_L is satisfied by the one component, ψ , of the vector potential.

We seek solutions for ϕ and ψ in the general forms

$$\varphi(r, \theta, t) = \left(\frac{r}{d}\right)^q f(t) \Omega_L(\alpha_L, \theta) d^2 \quad (2.18)$$

$$\psi(r, \theta, t) = \left(\frac{r}{d}\right)^q f(t) \Omega_T(\alpha_T, \theta) d^2 \quad (2.19)$$

where

$$\alpha_L = \frac{v(t)}{c_L}, \quad \alpha_T = \frac{v(t)}{c_T}, \quad (2.20a, b)$$

and d is a length parameter. Substituting Eq. (2.18) into $\nabla^2 \omega = \dot{\omega}/c_L^2$, multiplying the result by r^{2-q} , and considering the limit $r \rightarrow 0$, the following equation for Ω_L is obtained

$$(1 - \alpha_L^2 \sin^2 \theta) \Omega_L'' - \alpha_L^2 (1 - q) \sin(2\theta) \Omega_L' + q \{ q + \alpha_L^2 [(2 - q) \cos^2 \theta - 1] \} \Omega_L = 0 \quad (2.21)$$

Here $\Omega_L' = d\Omega_L(\alpha_L, \theta)/d\theta$. An analogous equation is obtained for $\Omega_T(\alpha_T, \theta)$. Following Ref. [11], a solution of Eq. (2.21) is sought of the form

$$\Omega_L(\alpha_L, \theta) = (1 - \alpha_L^2 \sin^2 \theta)^{q/2} \Omega_L^*(\alpha_L, \theta) \quad (2.22)$$

Substitution of Eq. (2.22) into Eq. (2.21) yields a much simpler equation for Ω_L^* , which can, however, be further simplified by introducing the variable ω_L by

$$\tan \omega_L = (1 - \alpha_L^2)^{1/2} \tan \theta \quad (2.23)$$

The solution of the resulting equation for Ω_L^* is

$$\Omega_L^* = A_L \sin(q\omega_L) + B_L \cos(q\omega_L) \quad (2.24)$$

A completely equivalent expression is obtained for Ω_T^* in terms of ω_T , where the definition of ω_T is equivalent to Eq. (2.23), and Ω_T is related to Ω_T^* by the equivalent of Eq. (2.24).

The displacement potentials (2.18) and (2.19) may be used to obtain the corresponding expressions for the displacements and the stresses. These results show that the near-tip fields separate into symmetric and antisymmetric parts. For the symmetric parts the boundary conditions at $\theta = \pi$, $r > 0$ yield two homogeneous equations for the constants B_L and A_T . The requirement that the determinant of the coefficients must vanish results in the equation

$$D(\alpha_L, \alpha_T) \sin(q\pi) \cos(q\pi) = 0 \quad (2.25)$$

where $D(\alpha_L, \alpha_T)$ is the well-known Rayleigh function:

$$D(\alpha_L, \alpha_T) = (\alpha_T^2 - 2)^2 - 4(1 - \alpha_T^2)^{1/2} (1 - \alpha_L^2)^{1/2} \quad (2.26)$$

Equation (2.25) is an equation for q . In order that the strain energy is integrable, we must have $q > 1$. For a velocity of crack propagation smaller than the Rayleigh wave velocity, the

smallest root q of Eq. (2.25) for which $\text{Re}(q)$ is greater than unity is $q = 3/2$. Details can be found in Ref. [11]. After some manipulation

$T_\theta^I(\theta, v)$ is obtained as

$$T_\theta^I(\theta, v) = \frac{(1 - \alpha_L^2)^{1/2} (2 - \alpha_T^2) \sqrt{2} \left\{ \frac{(2 - \alpha_L^2) \cos 2\theta + \alpha_L^2 - \alpha_T^2}{2(1 - \alpha_L^2)^{1/2}} \right.}{D(\alpha_L, \alpha_T)} \times \Omega_{L2} - \frac{2(1 - \alpha_T^2)^{1/2} \cos 2\theta}{2 - \alpha_T^2} \Omega_{T2} + (\Omega_{L1} - \Omega_{T1}) \sin 2\theta \quad (2.27)$$

where

$$\Omega_{T1} = \left[\frac{(1 - \alpha_T^2 \sin^2 \theta)^{1/2} - \cos \theta}{1 - \alpha_T^2 \sin^2 \theta} \right]^{1/2} \quad (2.28)$$

$$\Omega_{T2} = \left[\frac{(1 - \alpha_T^2 \sin^2 \theta)^{1/2} + \cos \theta}{1 - \alpha_T^2 \sin^2 \theta} \right]^{1/2} \quad (2.29)$$

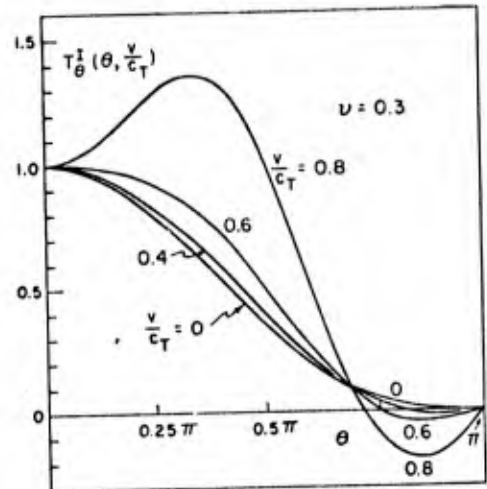


FIGURE 3: Function $T_\theta^I(\theta, v)$ versus θ for various values of v/c_T .

The expressions for Ω_{L1} and Ω_{L2} are obtained from Eqs. (2.28) and (2.29) by replacing subscripts T by L. For various values of v/c_T , the function $T_\theta^I(\theta, v)$ is plotted versus θ in Fig. 3. The expression given by Eq. (2.27) agrees with the one obtained by Yoffe [12] and Baker [13] for special problems. It is of note that the maximum value of $T_\theta^I(\theta, v)$ moves out of the plane $\theta = 0$ (the plane of crack propagation) as v increases beyond a critical value.

For a crack propagating with velocity $v(t)$ in a field of anti-plane strain we find

$$\tau_{\theta 3}(\theta, v) = \frac{1}{\sqrt{2}} \left\{ (1 - \alpha_T^2)^{-\frac{1}{2}} \Omega_{T1} \sin \theta + \Omega_{T2} \cos \theta \right\} \quad (2.30)$$

where Ω_{T1} and Ω_{T2} are defined by Eqs. (2.28) and (2.29). It can be checked that Eqs. (2.27) and (2.30) reduce to (2.15) and (2.16), respectively, in the limit $v \rightarrow 0$.

Near-tip expressions for the displacements can be obtained similarly.

2.4 Functions $k_I(t)$ and $k_{III}(t)$

Elastodynamic fields near a stationary crack tip can be generated by incident waves, or by loading of the fracture surface. A number of solutions for a semi-infinite crack were obtained by de Hoop [14]. The simplest of these is the near-tip stress field $\tau_{\theta 3}$ generated by a step-stress anti-plane shear wave of magnitude τ_0 , and angle of incidence α . The details of the analysis, which employs integral transform techniques and the Wiener-Hopf method, can also be found in Ref. [1], p. 372. The result is that near the crack tip $\tau_{\theta 3}$ is of the general form $\tau_{\theta 3} =$

$$(2\pi)^{-\frac{1}{2}} r^{-\frac{1}{2}} k_{III}(t) T_{\theta 3}^{III}(\theta) \quad \text{where } T_{\theta 3}^{III}(\theta) \text{ is defined by Eq. (2.16), and } k_{III}(t) \text{ is given by}$$

$$k_{III}(t) = 4\tau_0 \left(\frac{c_T}{\pi} \right)^{\frac{1}{2}} (\sin \frac{1}{2}\alpha) t^{\frac{1}{2}} \quad (2.31)$$

Thus, the stress intensity factor increases with time. If the crack is of finite length $2a$, the stress intensity factor increases until a wave diffracted from the opposite crack tip arrives. It is of interest that for the case of a step-stress wave the dynamic stress intensity factor shows an overshoot of $4/\pi - 1$ as compared to the stress intensity factor of the corresponding quasi-static problem. Details of this computation are given in Ref. [4]. It should of course be noted that the dynamic overshoot is smaller for a less rapid increase of the stress at the wavefront.

Stress intensity factors for diffraction of a longitudinal wave by a crack of finite length were computed by Thau and Lu [15]. The results presented in Ref. [15] are valid from the instant the incident wave arrives at the crack tip until a diffracted longitudinal wave reaches the opposite crack tip, is rediffracted, and then returns to the original tip, i.e., during two crack width transit times of a longitudinal wave. The peak value of $k_I(t)$ was found to be 30 per cent greater than the analogous static factor K_I .

If solutions are desired for longer times, or if additional boundaries are present, analytical approaches become too cumbersome, and it is necessary to resort to numerical methods, either finite element or finite difference methods.

In Ref. [16] elastodynamic stress intensity factors were computed by the finite element technique. It was found that crack tip elements with a singular strain field (singular elements) are less effective in elastodynamics than in elastostatics. A non-singular (ordinary) crack tip element whose crack-opening displacement is calibrated was found to be most effective. Detailed studies were also carried out in Ref. [16] of implicit and explicit time-step algorithms, proper sizes of elements, methods for solving equations systems, questions of non-reflecting boundaries, lumping of mass matrices and elimination of spurious oscillations superimposed on the correct solution. For a crack in a plate of finite width, subjected to an incident step-stress wave, computations of $k_I(t)$ by the finite element

method were presented by Anderson et al [17]. Finite difference methods were used for the same problem by Chen [18]. The results of Refs. [17] and [18] are summarized in Fig. 4, and they are compared with results obtained by Glazik [19], who used the calibrated element of Ref. [16]. It is noted that the ratio $k_I(t)/K_I(t)$ can run as high as three.

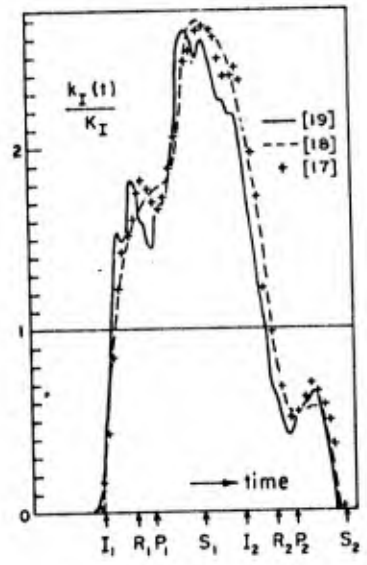


FIGURE 4: Elastodynamic stress intensity factor for a crack in a sheet of finite width. I_1 denotes arrival time of incident wave; $R_1 - I_1$ denotes time for Rayleigh wave to travel between crack tips; $P_1 - I_1$ and $S_1 - I_1$ denote times for diffracted P- and S- waves to travel to the nearest free surface of the sheet and back; I_2 denotes time for wave to travel length of sheet and back to the crack.

A solution of utility for superposition purposes, namely, the elastodynamic stress intensity factor due to suddenly applied concentrated forces on the crack surfaces was derived by Freund [20]. If the elastodynamic displacement field and stress intensity factor are known, as functions of crack length, for any symmetrical distribution of time-varying forces, then the stress

intensity factor due to any other symmetrical load system whatsoever acting on the same body, may be directly determined by a formula derived by Freund and Rice [21].

2.5 Functions $k_I(t, v)$ and $k_{III}(t, v)$

The computation of elastodynamic stress intensity factors for a rapidly propagating semi-infinite crack was reviewed by Achenbach [4]. Two cases should be considered separately, namely, the cases that the crack propagates under the influence of incident waves, or under the influence of a pre-existing quasi-static stress field.

Suppose that a cracked body is in equilibrium under applied loads. The loads are increased gradually, until a critical state is reached, and fracture is initiated. At the instant of fracture, the stresses in the plane of the crack are known from a quasi-static analysis. Let us consider the case that the only stress in the plane of the crack just prior to fracture is $\tau_{22} = p(x_1)$. The time of fracture initiation is taken as $t = 0$. It is assumed that the crack propagates in its own plane, and that the fracture process is so fast that in-plane wave motions are generated in the solid. For $t > 0$ the crack tip is located at $x_1 = X(t)$, where dX/dt is smaller than the velocity of Rayleigh waves. The propagation of the crack generates cylindrical waves. The elastodynamic fields are obtained by superimposing on the elastostatic field a solution to Eqs. (1.1)-(1.6) for a solid containing a slit $x_1 < X(t)$, with the following boundary conditions.

$$0 < x_1 < X(t) : \tau_{22} = -p(x_1) \quad (2.32)$$

$$-\infty < x_1 < 0 : \tau_{22} = 0 \quad (2.33)$$

$$-\infty < x_1 < \infty : \tau_{21} = 0 \quad (2.34)$$

$$x_1 \geq X(t) : u_2 = 0 \quad (2.35)$$

The initial conditions which complete the statement of the problem are that all field variables are zero prior to time $t = 0$. By superimposing this elastodynamic solution on the initial elastostatic solution, the fracture surface defined by $x_2 = 0$, $0 < x_1 < X(t)$ is rendered free of tractions.

The stress intensity factor for the problem stated above was obtained by Freund [22], in two steps. First the problem was solved for constant crack propagation velocity $dX/dt = v$. The complete elastic field for this problem can be solved by integral transform methods as discussed in Ref. [4]. By an ingenious argument Freund subsequently showed that $k_I(t, dX/dt)$ for the non-uniformly propagating crack can be obtained from the corresponding value for crack propagation at a constant velocity v , simply by replacing v by dX/dt , and vt by $X(t)$. This results in an expression of the form

$$k_I(t, \frac{dX}{dt}) = \left(\frac{2}{\pi}\right)^{\frac{1}{2}} k_2\left(\frac{dX}{dt}\right) \int_0^{X(t)} \frac{p(s) ds}{[X(t)-s]^{\frac{1}{2}}} \quad (2.36)$$

Here $k_2(dX/dt)$ is a complicated function of dX/dt . It is of interest to compare Eq. (2.36) with the corresponding expression for quasi-static fracture.

$$K_I(t) = \left(\frac{2}{\pi}\right)^{\frac{1}{2}} \int_0^{X(t)} \frac{p(s) ds}{[X(t)-s]^{\frac{1}{2}}} \quad (2.37)$$

Note that the elastodynamic and elastostatic stress intensity factors differ only by a multiplying function, which depends on dX/dt only. Crack propagation with variable velocity was also studied by Kostrov [23] by a direct method, which verified the result obtained by Freund.

Analogous results for the anti-plane case are discussed in Ref. [4]. It is found that

$$k_{III}(t, \frac{dX}{dt}) = k_{23}\left(\frac{dX}{dt}\right) K_{III}(t) \quad (2.38)$$

where

$$k_{23}\left(\frac{dX}{dt}\right) = \left[1 - \frac{1}{c_T} \frac{dX}{dt}\right]^{\frac{1}{2}} \quad (2.39)$$

The functions $k_2(dX/dt)$ and $k_{23}(dX/dt)$ have been plotted in Fig. 5, for a material with Poisson's ratio $\nu = 0.25$. The stress-intensity factors vanish for cracks propagating with velocities c_R and c_T , respectively, where c_R is the velocity of Rayleigh waves.

Elastodynamic fields for a crack expanding with a constant velocity from a single point in a uniform stress field can be treated rigorously. The plane strain

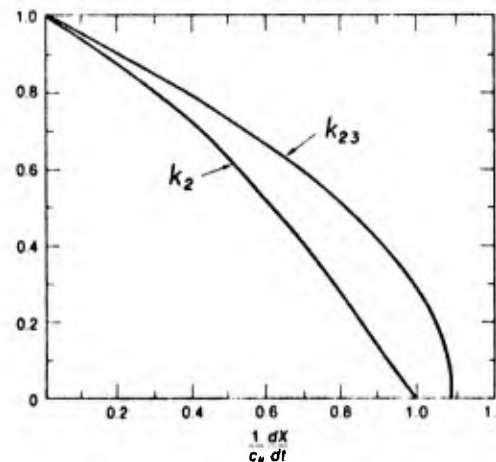


FIGURE 5: Ratios of elastodynamic to elastostatic stress intensity factors.

case was analyzed by Broberg [24]. Stress distributions in the plane of the crack for Broberg's problem were presented by Kamei and Yokobori [25]. For expanding central cracks certain field variables are self-similar, which introduces a considerable simplification in the analysis. Self-similar solutions are discussed in more detail later in this paper. Expanding penny-shaped and elliptical cracks were discussed by Willis [26], who also listed additional references for self-similar solutions.

It is somewhat more complicated to analyze near-tip fields at a crack tip running under the influence of incident waves. Some available solutions have been reviewed in Ref. [4].

2.6 Cracks Propagating in and near Interfaces

For elastostatic problems the nature of the singularity near the tip of a crack in the interface of two bonded dissimilar half planes was analyzed by Williams [27]. Williams was apparently the first to discover that for in-plane problems the singular parts of the near-tip stresses show intense oscillations, while the displacements on the crack surfaces interpenetrate. Mathematically the oscillating singularities appear, because the factor p in the asymptotic expressions given by Eq. (2.11) turns out to be a complex number. The same situation prevails for elastodynamic problems of rapidly propagating interface flaws, as shown in Ref. [28]. Available solutions for elastodynamic stress intensity factors for crack tips propagating in interfaces or normal to interfaces have recently been reviewed by Atkinson [29].

2.7 Experimental Results

What appears to be the first recorded experimental work on fracture under dynamic loading conditions was carried out by J. Hopkinson. Hopkinson measured the strength of steel wires when they were suddenly stretched by a falling weight. He explained the results in terms of elastic waves propagating up and down the wire. The next significant investigation was carried out by B. Hopkinson, who detonated an explosive charge in contact with a metal plate. In his work, B. Hopkinson demonstrated the effect of "spalling" or "scabbing," which occurs when the compressive pulse generated by the explosive is reflected at the opposite side of the plate as a tensile pulse. The reflected pulse produces tensile fractures, and a disk of metal roughly in the shape of a spherical cap breaks away from the surface directly opposite the explosive charge. After the work of B. Hopkinson very little research was apparently carried out in this area until the Second World War. Kolsky [30] devoted a chapter of his book to fractures produced by stress waves, in which the work of J. and B. Hopkinson is described and further work dating from the late forties and the early fifties is discussed.

In recent years much additional experimental work has been carried out with a large number of materials and with specimens of various geometrical configurations. The stress pulses were produced by the ballistic impact of projectiles or by explosive charges. In a review article on stress waves and fracture, Kolsky and Rader [31] describe many of these investigations. Extensive investigations on the fracture of glass under dynamic loading conditions are discussed in the book by Kerkhof [32]. Experimental work of recent vintage was reported at a 1972 conference on dynamic crack propagation, and was published in the proceedings [33]. Interest in fracture under dynamic loading conditions is now increasing rapidly. The proceedings of the 12th annual meeting of the Society of Engineering Science contain a relatively large number of experimental studies on dynamic fracture [34].

In Ref. [35] a new method was reported of experimentally investigating the behavior of a crack in a stress wave environment. The method was used to study the initial stages of dynamic crack propagation in Homalite 100, a polyester. The experimental method employs an electromagnetic loading device, and it permitted the application of pressure pulses to the surfaces of an 18 inch crack. The amplitude (51 psi to 1020 psi) and duration ($\sim 200 \mu\text{sec}$) of the pulses were highly repeatable. A high speed framing camera, synchronized with the loading device, was used to record the time required for the crack to begin to propagate and its subsequent extension and velocity.

3. FRACTURE MECHANICS CONSIDERATIONS

Fracture mechanics is concerned with the computation of the fields of stress and deformation around a crack, and with conditions for growth of the crack. It provides the necessary framework for analysis on the macroscopic level. A fracture mechanics problem consists of two parts: a certain amount of stress analysis is followed by an application of a fracture criterion. In the stress analysis part mathematical idealizations are introduced. An infinitesimally thin crack and linearized theory together give rise to the square-root-singularities discussed in the previous section. The fracture criterion generally is an inequality which provides a necessary condition for the onset of crack propagation.

Fracture mechanics started with the work of A. A. Griffith in the early twenties. Thirteen congresses ago, at this same University, during the First Congress of Theoretical and Applied Mechanics, Griffith presented a paper in which he stated, "If owing to the action of a stress a pre-existing crack is caused to extend, a quantity of energy proportional to the area of the new surface must be added, and the condition that this shall be possible is that such addition of energy shall take place without any increase of the total potential energy of the system." This means that the increase of

potential energy due to the surface tension of the crack must be balanced by the decrease in the potential of the strain energy and the applied forces. In mathematical terms we have for Mode I, plane strain, and symmetric extension:

$$\frac{dU}{da} = 4\Gamma_F \quad (3.1)$$

Here U is the total potential of strain energy and applied forces per unit thickness, $2a$ is the length of the crack, and Γ_F is the specific surface energy per unit surface area. Thus, mechanical energy of the body is "dissipated" during the fracture process, even though the material is perfectly elastic. The loss of mechanical energy as new fracture surface is formed becomes plausible if we consider the work of the internal (cohesive) forces that are removed as new fracture surface, which is free of tractions is formed. Since the cohesive tractions that are removed are opposite in direction to the relative displacements of the newly formed fracture surfaces, their work is negative. Thus, in the course of crack propagation mechanical energy is extracted from the body. Within the idealized framework of linearized continuum mechanics the region over which cohesive tractions are released as the crack propagates is infinitesimal, namely, the tip of the propagating crack. Nevertheless the energy release rate has a finite value because of the presence of square-root terms in the field variables which enter in the energy release rate. It was shown by Irwin that the energy release rate may be expressed in the form (Mode I, plane strain)

$$\frac{dU}{da} = G = \frac{1-\nu}{2\mu} [K_I]^2 \quad (3.2)$$

Strictly Eq. (3.1) may be applied only to materials which do not suffer non-linear effects prior to fracture. However, about twenty-five years after Griffith's original contribution, Irwin and Orowan suggested a modification to accommodate limited plastic deformation near the crack tip. They replaced the surface energy term Γ_F by a term Γ_E which includes the energy of plastic distortion absorbed by the fracture process. Irwin noted that a precise interpretation of the term Γ_E is unnecessarily restrictive. Provided the plastic zone is small, a theory for correlating fracture behavior can be substantiated. In his view the modified theory consists in evaluating the rate of strain energy release at the point of fracture. If the fracture process is essentially similar for different loadings and geometries, the fracture event occurs when the strain energy release rate reaches a critical value. This critical value can be regarded as a material property, i.e., Γ_E , to be determined by a fracture test.

The energy release rate, G , and the flux of energy into the crack tip, F , are related by $F = G dX/dt$. For elastodynamic problems where time enters as an independent variable, it is

quite simple to compute the flux of energy into the moving crack tip. A detailed discussion can be found in Ref. [4], as well as in the papers by Atkinson and Eshelby [36], Kostrov and Nikitin [37] and by Freund [38]. In the vicinity of the crack tip we write

$$\tau_{2j}(x_1, 0, t) = \frac{T_{2j}}{[x_1 - X(t-t_f)]^{1/2}} \quad (3.3)$$

$$\dot{u}_j(x_1, 0^\pm, t) = \frac{\dot{u}_j^\pm}{[X(t-t_f) - x_1]^{1/2}} \quad (3.4)$$

where the fracture process is assumed to start at time $t = t_f$, i.e., $X(t) \equiv 0$ for $t \leq t_f$, and the \pm signs relate to $x_2 = 0^+$ and $x_2 = 0^-$, respectively. The flux of energy into the crack tip then is

$$F = -\frac{\pi}{2} T_{2j} [\dot{u}_j^- - \dot{u}_j^+] \quad (3.5)$$

The obvious advantage of Eq. (3.5) is that only the field variables in the plane of fracture and near the crack tip need be computed to obtain a fracture criterion. By comparison with Eqs. (2.3)-(2.6) the relations between T_{2j} and $k_{I,II,III}(t, dX/dt)$ can immediately be established. Similarly \dot{u}_j^\pm can be expressed in terms of $k_{I,II,III}(t, dX/dt)$. Thus, the only quantities which need to be computed are the stress intensity factors, and Eq. (3.5) can be expressed as

$$F = -\frac{v^3}{2\mu c_T^2 D(\alpha_L, \alpha_T)} \left\{ (1-\alpha_L^2)^{1/2} [k_I(t, v)]^2 + (1-\alpha_T^2)^{1/2} [k_{II}(t, v)]^2 \right\} + \frac{v}{2\mu(1-\alpha_T^2)^{1/2}} [k_{III}(t, v)]^2 \quad (3.6)$$

where $D(\alpha_L, \alpha_T)$ is defined by Eq. (2.26). In terms of the flux of energy into the crack tip the necessary condition for fracture is

$$F = 2\Gamma \frac{dX}{dt} \quad (3.7)$$

where Γ may be either Γ_F or Γ_E . It should be noted that Γ may depend on dX/dt .

It is relatively simple to apply Eq. (3.7) for the case of anti-plane shear, to investigate the generation of crack propagation by an incident step stress wave of the form

$$u_3 = \int_0^{c_T t + x_1 \sin\alpha - x_2 \cos\alpha} g(v) dv \quad (3.8)$$

where $u_3 \equiv 0$ for $c_T t + x_1 \sin\alpha - x_2 \cos\alpha \leq 0$. The wave strikes the crack tip at time $t = 0$, and

α is the angle of incidence. Suppose the crack tip starts to propagate at time $t = t_f$. The stress intensity factor follows from results stated in Ref. [4] as

$$k_{III}\left(t, \frac{dX}{dt}\right) = -\mu \left(\frac{2}{\pi}\right)^{\frac{1}{2}} (1-\sin\alpha)^{\frac{1}{2}} \left[1 - \frac{1}{c_T} \frac{dX}{dt}\right]^{\frac{1}{2}} I(t) \quad (3.9)$$

where

$$I(t) = \int_0^{c_T t + X(t-t_f)\sin\alpha} \frac{g(\zeta) d\zeta}{[c_T t + X(t-t_f)\sin\alpha - \zeta]^{\frac{1}{2}}} \quad (3.10)$$

By employing Eq. (3.8) and Eq. (3.6), F is computed, and Eq. (3.7) subsequently yields

$$\frac{\mu}{\pi} (1-\sin\alpha) \left\{ \frac{c_T - dX/dt}{c_T + dX/dt} \right\}^{\frac{1}{2}} [I(t)]^2 = 2\Gamma \quad (3.11)$$

This relation can be used to compute both t_f and dX/dt .

Let us consider the special case of a step incident wave defined by $g(s) = \tau_o/\mu$. From the condition that both $dX/dt \equiv 0$ and $X(t-t_f) \equiv 0$ just prior to time $t = t_f$ we obtain

$$t_f = \frac{\pi\mu\Gamma}{2(1-\sin\alpha)c_T\tau_o^2} \quad (3.12)$$

Thus, there is an incubation time before fracture starts. The incubation time is just the time required by $k_{III}(t)$ to reach a critical value which is the same as for the quasi-static case.

For $t > t_f$, Eq. (3.11) provides an equation for dX/dt , which can easily be solved if it is assumed that Γ is constant. For the case $\alpha = 0$, i.e., when the wavefront is parallel to the crack, we obtain for $t \geq t_f$

$$\frac{1}{c_T} \frac{dX}{dt} = \frac{(2\tau_o^2)^2 t^2 - (\pi\mu\Gamma/c_T)^2}{(2\tau_o^2)^2 t^2 + (\pi\mu\Gamma/c_T)^2} \quad (3.13)$$

It is noted that $dX/dt \rightarrow c_T$ as $t \rightarrow \infty$.

Similar computations can be carried out for the in-plane case, as discussed by Freund [5] except that it is not possible to obtain simple closed form expressions.

4. SELF-SIMILAR ELASTODYNAMIC SOLUTIONS

For two-dimensional elastodynamic problems without a characteristic length, and for appropriate conditions on the boundaries, some of the field variables are self-similar. Let $\sigma(r, \theta, t)$ be a

solution of the two-dimensional wave equation $\nabla^2 \sigma = (1/c)^2 \ddot{\sigma}$. If $\sigma(r, \theta, t)$ is self-similar, it will depend on θ and the ratio r/t , rather than on θ and r and t separately.

To determine $\sigma(r/t, \theta)$ it is convenient to introduce the new variable $s = r/t$. The equation governing $\sigma(s, \theta)$ follows as

$$s^2 \left(1 - \frac{s^2}{c^2}\right) \frac{\partial^2 \sigma}{\partial s^2} + s \left(1 - \frac{2s^2}{c^2}\right) \frac{\partial \sigma}{\partial s} + \frac{\partial^2 \sigma}{\partial \theta^2} = 0 \quad (4.1)$$

For $s \leq c$, Eq. (4.1) is elliptic. By means of Chaplygin's transformation

$$\beta = \text{arc cosh}(c/s) \quad (4.2)$$

where $\beta \geq 0$, Eq. (4.1) can be simplified to Laplace's equation $\partial^2 \sigma / \partial \beta^2 + \partial^2 \sigma / \partial \theta^2 = 0$. The domain in the β - θ plane generally is a semi-infinite strip. In this domain we have $\sigma = \text{Re}[\Sigma(\gamma)]$, where $\gamma = \beta + i\theta$. It is often convenient to map the strip in a half-plane, $\zeta = \xi + i\eta$, by a conformal mapping $\gamma = \omega(\zeta)$, and to determine an analytic function in the ζ -plane which satisfies appropriately transformed boundary conditions along the real axis. Details can be found in Ref. [1], p. 154.

For $s > c$, Eq. (4.1) is hyperbolic. It can be checked that through the transformation

$$\alpha = \text{arc cos}(c/s) \quad (4.3)$$

Eq. (4.1) reduces to the one-dimensional wave equation with solutions

$$\sigma = \Omega_+(\alpha + \theta) + \Omega_-(\alpha - \theta) \quad (4.4)$$

where Ω_{\pm} are arbitrary functions of the characteristic variables $\alpha \pm \theta$. In the s - θ plane the characteristics are tangents to the circle defined by $s = c$.

For elastodynamic problems the method of self-similar solutions was used by Miles [39]. The method was also discussed by Willis [26]. An equivalent method was developed in the early 1930's by U.I. Smirnov and S. L. Sobolev. A general discussion of that method as well as a few examples can be found in the book by Smirnov [40]. Recently a review with several applications was given by Cherepanov and Afanasev [41].

4.1 An Elastodynamic Solution for a Wedge

One of the still essentially unsolved problems in elastodynamic theory concerns a wedge of angle $\pi\pi$, whose surfaces are subjected to arbitrary disturbances. A review of attempts to obtain rigorous solutions was given by Knopoff [42]. Only boundary conditions of smooth contact with rigid planes have allowed an exact solution, which was derived by Kostrov [43]. In this section we briefly indicate the construction of a self-similar elastodynamic solution for a wedge-shaped region with certain

conditions on the surface tractions. The suitability of the method of self-similar solutions for wedge shaped regions was already shown in Ref. [44] for the case of anti-plane strain. Applications to cases of skew crack propagation and crack bifurcation are discussed in later sections.

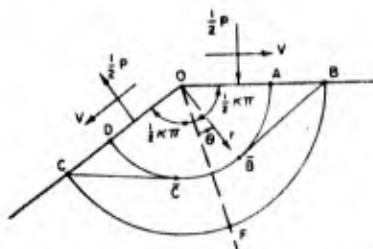


FIGURE 6: Moving loads on an elastic wedge.

Suppose a wedge is subjected to a line load normal to one of the surfaces. The load is applied at time $t = 0$ at the vertex, and then moves with a constant velocity V away from the vertex. The problem can be separated into a symmetrical and an antisymmetrical problem. Here we will consider the antisymmetrical problem shown in Fig. 6. The boundary conditions are

$$r > 0, \theta = \pm \frac{1}{2}\pi: \quad \tau_{\theta r} = 0 \quad (4.5)$$

$$\tau_{\theta} = \mp P\delta(r-Vt) \quad (4.6)$$

The wedge is at rest prior to time $t = 0$. The pattern of waves for $t > 0$ is shown in Fig. 6. For these boundary conditions the time derivatives of the displacement potentials are self-similar.

Following the steps outline earlier, we obtain $\phi(\beta_L, \theta)$ and $\psi(\beta_T, \theta)$ in domains $\beta_L \geq 0, -\frac{1}{2}\pi \leq \theta \leq \frac{1}{2}\pi$ and $\beta_T \geq 0, -\frac{1}{2}\pi \leq \theta \leq \frac{1}{2}\pi$, respectively. These domains are the mappings of OBCD and OABED, respectively. Here β_L and β_T follow from Eq. (4.2) by inserting $c = c_L$ and $c = c_T$, respectively. In the domains corresponding to ABE and DCE we obtain wave equations, with solutions which are analogous to Eq. (4.4), but with α_T and θ as independent variables. Here α_T is defined by Eq. (4.3), with c_T for c . The boundary conditions (4.5) and (4.6) provide the appropriate relations between the derivatives of ϕ and ψ along the boundaries of the two semi-infinite strips. Next we proceed to map the two strips on half-planes by means of mappings

$$\cosh\left(\frac{Y_L}{\kappa} + i\frac{\pi}{2}\right) = \frac{1}{\zeta_L}, \quad \cosh\left(\frac{Y_T}{\kappa} + i\frac{\pi}{2}\right) = \frac{1}{\zeta_T}$$

The analytic functions in the ζ_L - and ζ_T -planes must satisfy coupling conditions along the real axes, which follow from the conditions along OB, AB, CD and OC in the physical plane. The details of the analysis are much too lengthy to be

presented here, but they will be available elsewhere. Let us just note that the formulation leads to a system of coupled singular integral equations with Cauchy kernels. A numerical scheme based on series expansions in terms of Chebyshev polynomials was developed to obtain numerical solutions. Some results for the particle velocity in the radial direction are shown in Fig. 7.

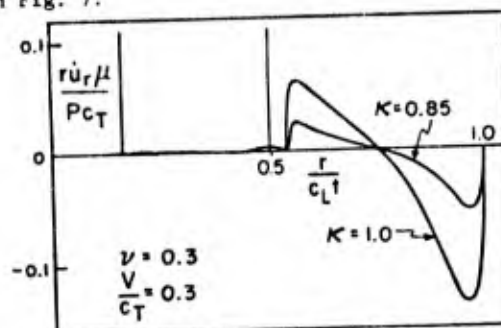


FIGURE 7: Particle velocity in the radial direction on a face of the wedge.

5. SKEW CRACK PROPAGATION AND CRACK BIFURCATION

If a homogeneous, isotropic, linearly elastic solid containing a plane crack is loaded so that the singular parts of the near-tip stresses are symmetric relative to the plane of the crack, one might perhaps expect the crack to propagate in its own plane. Experiments often show, however, skew crack propagation and crack bifurcation, especially for essentially brittle fracture. Although it has been suggested that elastodynamic effects play an important role in these phenomena, some first analytical investigations for the case of anti-plane strain, have only been published recently, see Refs. [45] and [46]. The computation of the elastodynamic fields presented the principal obstacle. It is shown here that the method of self-similar solutions provides a powerful tool for the analysis of elastodynamic skew crack propagation and crack bifurcation.

5.1. Skew Crack Propagation in Anti-Plane Strain

A way to employ self-similarity of field variables for the computation of elastodynamic near-tip stress fields in anti-plane strain, for the case that a semi-infinite crack propagates out of its own plane was devised by Achenbach and Varatharajulu [45]. Here we will employ the results of Ref. [45] to explore an elastodynamic explanation of skew crack propagation under stress-wave loading. A two-dimensional geometry is considered. An unbounded body containing a semi-infinite crack ($x_2=0, x_1 \geq 0, -\infty < x_3 < \infty$) is subjected to a suddenly applied anti-plane line load at $x_1 = 0, x_2 = -a$. The load generates a stress wave, which strikes the crack tip. By employing analytical results of Ref. [45] in conjunction with the fracture criterion of the balance of rates of energies, the necessary

condition for skew crack propagation at the instant that the crack is struck is investigated.

Let us first investigate the elastodynamic fields which are generated when a branch emanates asymmetrically from the tip of a semi-infinite crack, when the crack is struck by a horizontally polarized shear wave, whose wavefront is parallel to the surfaces of the semi-infinite crack. The reflection and diffraction of the incident wave gives rise to a plane wave and a diffracted cylindrical wave centered at the original crack tip. It is assumed that the semi-infinite crack propagates at the instant that the crack is struck, at an angle $\kappa\pi$, and with velocity v , where $v/c_T < 1$. At time $t > 0$, the crack tip is

located at point D. The pattern of wavefronts and the position of the crack tip are shown in Fig. 8. The particle velocity of the incident wave is of the form $H(t-x_2/c_T)$, where $H(\)$ is the Heaviside step function. For this problem the particle velocity is self-similar, and the analysis proceeds as outlined at the beginning of section 4. Details can be found in Ref. [45].

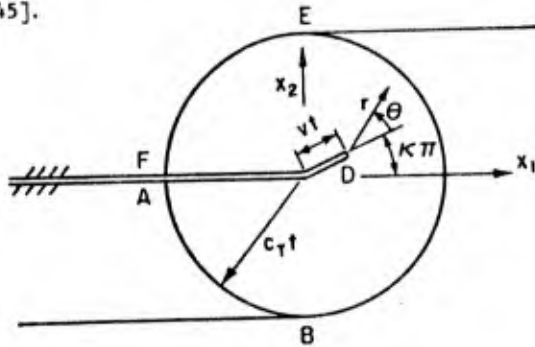


FIGURE 8: Pattern of wavefronts and position of crack tip for skew crack propagation under the influence of a step-stress wave.

Relative to a system of moving coordinates shown in Fig. 8, we find for small values of r :

$$\tau_{\theta 3} \sim (2\pi)^{-\frac{1}{2}} r^{-\frac{1}{2}} k_{III}(t, v, \kappa) T_{\theta 3}^{III}(\theta, v) \quad (5.1)$$

where $T_{\theta 3}^{III}(\theta, v)$ is defined by Eq. (2.30), and

$$k_{III}(t, v, \kappa) = 2\pi^{\frac{1}{2}} \left(1 - \frac{v}{2}\right)^{\frac{1}{2}} \left(\frac{t}{v}\right)^{\frac{1}{2}} K(\kappa) \quad (5.2)$$

$$K(\kappa) = \mu F'(\xi_D) / [\omega''(\xi_D)]^{\frac{1}{2}} \quad (5.3)$$

In Eq. (5.3), ξ_D is the mapping of the point D in the $\zeta = \xi + i\eta$ plane, and $\omega(\zeta)$ defines the Schwarz-Christoffel transformation, $\gamma = \omega(\zeta)$, from the $\gamma = \beta + i\theta$ plane to the ζ -plane. The real part of $F(\zeta)$ defines the particle velocity of the cylindrical diffracted wave.

Let us now return to the problem of the concentrated line load. Relative to a system of cylindrical coordinates centered at $x_1 = 0$, $x_2 = -a$, the stress wave due to an anti-plane line load of P force units per unit length can be found in Ref. [1], p. 157. Assuming that the distance a is large, the wave arriving at the plane of the crack can be considered a plane wave. For small values of $\bar{t} = t - a/c_T$ we then have relative to coordinate system centered at the crack tip:

$$(\dot{u}_3)_{inc} = \frac{P}{2\pi\rho} c_T^{-3/2} (2a)^{-\frac{1}{2}} (\bar{t} - x_2/c_T)^{-\frac{1}{2}} H(\bar{t} - x_2/c_T) \quad (5.4)$$

When the wave given by Eq. (5.4) strikes the crack a reflected and a diffracted wave are generated. Apart from the time dependence, the above elastodynamic problem is precisely the one discussed earlier in this section. Taking into account that superposition can be employed in the limit $\bar{t} = 0$, $\tau_{\theta 3}$ for small time is given by Eq. (5.1) where

$$k_{III}(t, v, \kappa) = \left(\frac{2\pi}{a}\right)^{\frac{1}{2}} \left(1 - \frac{v}{2}\right)^{\frac{1}{2}} \left(\frac{c_T}{v}\right)^{\frac{1}{2}} \frac{P}{4\mu} K(\kappa) \quad (5.5)$$

The flux of energy into the propagating crack tip follows from the last term of Eq. (3.6). For the problem at hand the function F is plotted in Fig. 4 of Ref. [47]. The noteworthy result is that the rate of energy flux into a propagating crack tip shows a maximum at $\kappa = 0$ only for values of v/c_T which are smaller than a value of v/c_T of approximately $v/c_T = 0.27$. Apparently the rate of energy flux into a crack tip can be higher for skew crack propagation than for a crack propagating in its own plane.

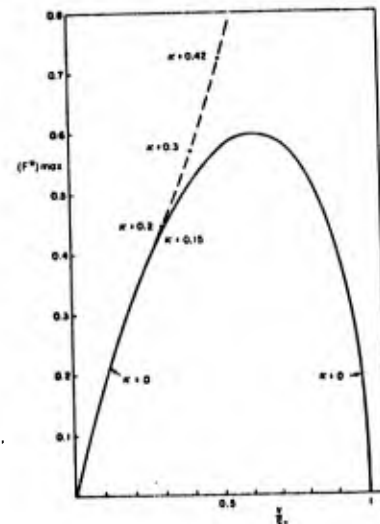


FIGURE 9: Maximums of F with respect to κ plotted vs. v/c_T ; $F^* = (16\pi a \mu / P^2 c_T) F$.

The tendency towards skew crack propagation can be examined on the basis of the balance of rates of energies. This fracture criterion is stated by Eq. (3.7). In the present problem we have $F = 2\Gamma v$. For essentially brittle fracture Γ is the specific surface energy, which is independent of κ . In a plot of F vs. κ and $2\Gamma v$ vs. κ for specific v/c_T , the term $2\Gamma v$ is then represented by a horizontal line. In accordance with the balance of rates of energies, the values of v and κ are determined by a point of intersection of the curves for F and $2\Gamma v$. Since both v and κ are as yet unknown an additional condition is required. Such an additional condition is that only an intersection where $2\Gamma v$ is tangent to F (i.e., F is a maximum with respect to κ) defines a case of stable crack propagation relative to variations of κ . Thus, in Fig. 9, the maxima of F with respect to κ have been replotted versus v/c_T , and values of κ at which the maximums of F are reached have been indicated. In this figure $2\Gamma v$ is a straight line through the origin. The intersection of $2\Gamma v$ and F defines a case of crack propagation and the pertinent values of v and κ follow from the point of intersection in Fig. 9. The foregoing discussion defines Γ and P as the principal quantities controlling skew crack propagation. For small enough Γ and/or P , $2\Gamma v$ is tangential to F at $\kappa = 0$, and thus v/c_T will be relatively small and the crack will propagate in its own plane. For larger values of Γ or P the relevant intersection is at $\kappa > 0$, i.e. skew crack propagation can be expected.

5.2 Bifurcation of a Running Crack in Anti-plane Strain

Once the propagation of a crack has started, the primary crack often bifurcates into two or more branches, each of which may propagate over a short distance, and then again split into two or more new branches. Crack bifurcation occurs in a variety of materials, and under different external conditions. The phenomenon is, however, particularly frequent for essentially brittle fracture, when the speed of crack propagation becomes relatively large. Experimental observations of the magnitude of the speed of crack propagation at branching suggest that elastodynamic effects play a significant role.

We take the view that bifurcation of a running crack is an instability phenomenon, and that a necessary condition for bifurcation can be determined by comparing states prior to branching and after branching has taken place. The comparison requires expressions for the elastodynamic fields near the tips of the branches. For symmetric bifurcation in anti-plane strain the near-tip fields were analyzed in Ref. [46], where a necessary condition for bifurcation of a running crack was also established on the basis of the balance of rates of energies.

The model problem considered here and in Ref. [46] concerns the two-dimensional geometry of

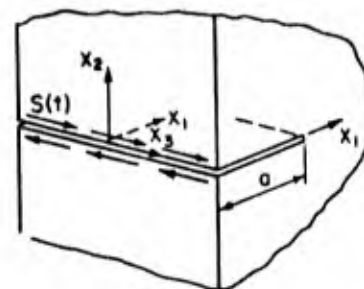


FIGURE 10: Tearing of an edge crack.

an edge crack of depth a in a semi-infinite elastic solid, as shown in Fig. 10. The body is subjected to a distribution of equal and opposite concentrated forces in the x_3 -direction, applied at $x_1 = 0$ and $x_2 \pm \epsilon$, where ϵ is very small. These anti-plane shear forces, of magnitude $S(t)$ force units per unit length, give rise to deformations in anti-plane strain. It is assumed that the fields of stress and deformation generated by $S(t)$ are elastostatic in nature.

Prior to crack propagation, the stress component τ_{23} in the plane $x_2 = 0$, and near $x_1 = a$, is given by

$$\tau_{23} = \left\{ \frac{1}{\pi} \left(\frac{2}{a} \right)^{\frac{1}{2}} \left(\frac{1}{x_1 - a} \right)^{\frac{1}{2}} + 0 \left[(x_1 - a)^{\frac{1}{2}} \right] \right\} S(t) \quad (5.6)$$

Let us now suppose that at time $t = 0$ a rapid Mode III tearing process starts, and that the crack begins to propagate, initially in its own plane, so that the position of the crack tip is defined by $x_1 = a + X(t)$, where $dX/dt < c_T$. It is assumed that the fields generated by the propagation of the crack are elastodynamic in nature. The propagation of a crack in its own plane has been analyzed in detail, see e.g. Ref. [4], at least for small times. Here we wish to consider the case that subsequent to propagation in its own plane in the time interval $0 < t < t_{bf}$,

the crack bifurcates symmetrically under angles $\pm \mu\pi$ from the points defined by $x_1 = a + X(t_{bf})$, as shown in Fig. 11. The elastodynamic fields generated by the removal of tractions from the crack branches and the subsequent application of the balance of rates of energies are the principal topics of analysis of Ref. [46].

In the initial stages, when the crack propagates in its own plane the stress intensity factor is

$$k_{III}(t, v) = 2 \left(\frac{1}{\pi a} \right)^{\frac{1}{2}} \left(1 - \frac{1}{c_T} \frac{dX}{dt} \right)^{\frac{1}{2}} S(t) \quad (5.7)$$

The flux of energy into the crack tip follows

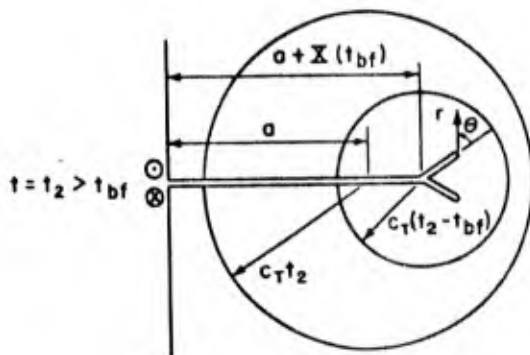


FIGURE 11: Rapid propagation and bifurcation in anti-plane strain of an edge crack.

from the last term of Eq. (3.6). The balance of rates of energies, Eq. (3.7), yields

$$\left(1 - \frac{1}{c_T} \frac{dX}{dt}\right)^{\frac{1}{2}} \left(1 + \frac{1}{c_T} \frac{dX}{dt}\right)^{-\frac{1}{2}} \frac{dX}{dt} = \frac{\pi \Gamma_{II} a}{[S(t)]^2} \frac{dX}{dt} \quad (5.8)$$

Equation (5.8) yields not only the critical magnitude of $S(t)$, but also dX/dt . Both sides of Eq. (5.8) are plotted in Fig. 12. The right hand side is a straight line through the origin, whose slope decreases as $S(t)$ increases. The necessary condition for fracture is satisfied when the straight line intersects the curve representing the left-hand side of Eq. (5.8), i.e., when

$$S(t) = S_{cr} = (\pi \mu \Gamma a)^{\frac{1}{2}} \quad (5.9)$$

The subsequent speed of crack propagation can easily be computed from Eq. (5.8). There will be an instantaneous speed of crack propagation if $S(t)$ exceeds S_{cr} at the instant that fracture starts.

The fields near the tips of the two branches are obtained in two stages. First we solve a problem for which the particle velocity is self-similar, and then these results are employed to compute the near-tip fields for the problem illustrated in Fig. 11. Relative to the system of polar coordinates at the crack tip, shown in Fig. 11, the result is

$$k_{III}(v, \kappa) = \left(\frac{2\pi}{a}\right)^{\frac{1}{2}} \left(1 - \frac{v^2}{c_T^2}\right)^{\frac{1}{2}} \left(\frac{c_T}{v}\right)^{\frac{1}{2}} K(\kappa) S(t_{bf}) \quad (5.10)$$

where v is the velocity of the bifurcated crack tips.

An explicit expression for $K(\kappa)$ is given as Eq. (3.41) in Ref. [46]. The flux of energy into a crack tip is

$$F = \frac{\pi}{\mu} \frac{c_T}{a} [K(\kappa)]^2 [S(t_{bf})]^2 \quad (5.11)$$

The conditions are right for crack bifurcation at time $t = t_{bf}$ with velocity v , if the balance of rates of energies, Eq. (5.11), can be satisfied, which implies

$$[\pi K(\kappa)]^2 = \frac{2\pi a \Gamma_{II} \mu}{[S(t_{bf})]^2} \frac{v}{c_T} \quad (5.12)$$

Since this equation contains two unknowns, namely v and κ , an additional condition is required. Such an additional condition is that only a point where F is a maximum with respect to κ defines a case of stable crack propagation relative to variations of κ . Thus in Fig. 12

the maxima of $[\pi K(\kappa)]^2$ with respect to κ have been replotted versus v/c_T .

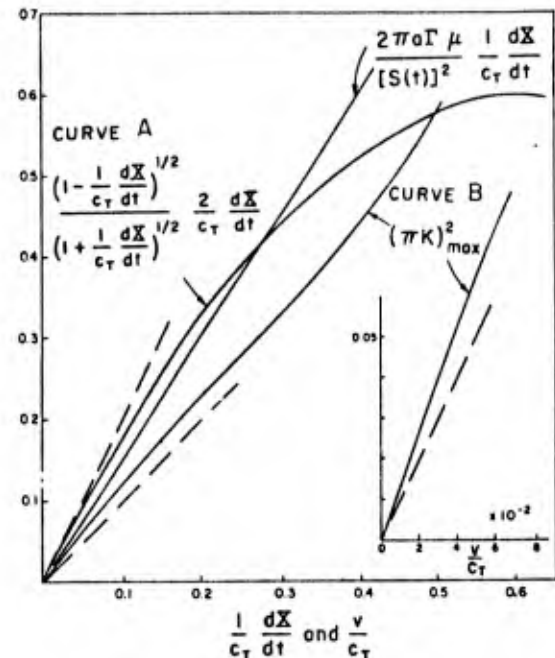


FIGURE 12: Terms appearing in the balance of rates of energies for propagation in the plane of the crack and for symmetric bifurcation.

When $S(t) = S_{cr} = (\pi \mu \Gamma a)^{\frac{1}{2}}$ the necessary condition for fracture is met. The load $S(t)$ may exceed S_{cr} before fracture in the plane of the crack may actually start. If that is the case there is an instantaneous speed of crack propagation, and subsequent values of dX/dt as $S(t)$ increases can be determined as the intersection of the line and the curve A, as previously discussed. From Fig. 12 we note, however, that as $S(t)$ increases, the straight line will eventually touch the curve

B for $[\pi K(\kappa)]_{\max}^2$, which is also plotted in Fig. 12. When that takes place Eq. (5.12) is satisfied, and the necessary condition for crack bifurcation is satisfied. The speed at which bifurcation takes place follows from the intersection of A with the straight line through the origin which touches the curve B. We find at the point of bifurcation $(1/c_T) dx/dt \sim 0.375$. This is the velocity of in-plane crack propagation at which the necessary condition for bifurcation is first met. The insert in Fig. 12 shows a somewhat enlarged view of the region for small v/c_T . The speed of bifurcation is found as $v/c_T \sim 0.02$.

The angle of bifurcation is $\kappa\pi \sim 0.22\pi$. Note that the speed of bifurcation is much smaller than the preceding in-plane crack propagation velocity. Once bifurcation has started the curve for propagation in the plane of the crack becomes, however, again operative, and the speed of crack propagation can increase rapidly until the condition is met for another bifurcation.

5.3 Bifurcation of a Running Crack for the In-Plane Case

Computations for deformation in anti-plane strain (Mode III) are of little significance for engineering problems. Anti-plane deformation is, however, of interest in a geophysical context. Solutions of anti-plane problems also frequently suggest the proper steps for the attack on in-plane problems. There are, however, some principal differences in the basic mechanisms of crack bifurcation for the anti-plane and in-plane cases, and these should be kept in mind. Branches of a primary crack under pure Mode-I loading generally are subjected to both Mode-I and Mode-II loading conditions. Mixed loading conditions do not occur for crack bifurcation in anti-plane strain.

The experimental information available in the literature is for in-plane deformation. It requires sophisticated high-speed photographic equipment to take a sequence of photographs showing the evolution of the pattern of bifurcating cracks. The techniques which were developed for this purpose are described by Kerkhof [32], p. 108. In Ref. [32] a number of shadow photographs of bifurcating cracks are shown, and numerical information on speeds of crack propagation is presented. A paper by Kalthof in Ref. [33], dealing with bifurcation of a primary edge crack in a stretched glass plate, includes a sequence of shadow photographs at a framing rate of 4 μ s, which is particularly illustrative of the first bifurcation of the primary crack. Experimental results were also reported in Refs. [48] - [51].

There are several differences between the experimental results for the in-plane case reported in the literature, and the analytical results for the anti-plane case obtained in the previous section. Experimentally the following angles were found for the in-plane case:

Congleton [48]: $\sim 20^\circ$; Clark, Irwin [49]: $\sim 17^\circ$; Kalthof [33]: $\sim 15^\circ$; Kobayashi et al [50]: $\sim 13^\circ$; Döll [51] measured the speed of the bifurcating branches as approximately 90% of the speed of the primary crack tip just prior to bifurcation. Kobayashi et al [50] found slightly smaller values. In the previous section the speed at which bifurcation of the primary crack tip can occur was obtained as 0.375 times the speed of transverse waves. For the in-plane case Kerkhof [32] measured a maximum crack velocity of approximately one third of the speed of longitudinal waves.

The differences between the analytical results for the anti-plane case presented in this paper and the experimental results for the in-plane case cited above can primarily be ascribed to differences in the basic fracture mechanisms. Another reason for the differences could be that in the analysis Γ (the crack extension energy) was assumed independent of the crack tip velocity. It has, however, been reported that experiments on steel under Mode-I loading show that for a rapidly propagating crack tip the crack extension energy may be more than a factor of ten higher than for slowly propagating crack tips. In principle it is not difficult to extend the analysis of the previous section to the case that Γ depends on the crack propagation velocity, but this would require an explicit expression for Γ in terms of the crack propagation velocity. There is no experimental information available for bifurcation in anti-plane strain, because this case is very difficult to achieve on a small test piece in a laboratory.

Clearly, it will be very interesting to obtain results analogous to the ones presented in Sections 5.1 and 5.2, for in-plane deformations. Work on these problems was in progress at the time of the writing of this article. In the analysis one first considers a case for which certain field variables are self-similar, and then one proceeds to use this solution in conjunction with superposition considerations for the loading conditions that are of interest. The solution of the self-similar problem is achieved along the lines sketched in Section 4. There are two wave equations, which can be reduced to Laplace's equations in semi-infinite strips containing slits. These strips are mapped on half-planes by means of Schwarz-Christoffel transformations. The conditions at the boundaries and at the wavefronts in the physical plane lead to a system of singular integral equations connecting the real and imaginary parts of analytic functions along the real axes of the half-planes. The system of singular integral equations is solved numerically by employing expansions in Chebyshev polynomials.

6 CONCLUDING REMARKS

The analysis of elastodynamic stress intensity factors is an essential part of investigations

dealing with the stability of cracks, when loads are applied at high rates, and when cracks may propagate rapidly as in essentially brittle fracture. In this paper some recent analytical and numerical results were discussed, within the context of the fracture criterion of the balance of rates of energies. At this stage of development of the subject, the emphasis has been on purely analytical work. There is, however, a growing interest in numerical and semi-numerical techniques, to deal with complicated geometries, and more general constitutive behavior of materials.

7. ACKNOWLEDGEMENT

This paper was prepared in the course of research sponsored by the Office of Naval Research under Contract ONR N00014-76-C-0063, and by the National Science Foundation under Grant No. ENG. 70-01465 A02. Dr. R. P. Khetan carried out the computations for Figures 3 and 7.

8. REFERENCES

1. J. D. Achenbach, Wave Propagation in Elastic Solids, North-Holland Publ. Co./American Elsevier, Amsterdam/New York, 1973.
2. Y.-H. Pao and C.-C. Mow, Diffraction of Elastic Waves and Dynamic Stress Concentrations, Crane Russak, New York, 1973.
3. A. C. Eringen and E. S. Suhubi, Elastodynamics, Vol. II, Linear Theory, Academic Press, New York, 1975.
4. J. D. Achenbach, "Dynamic Effects in Brittle Fracture," Mechanics Today, Vol. I (S. Nemat-Nasser, editor), Pergamon, New York 1974, p. 1.
5. L. B. Freund, "The Analysis of Elastodynamic Crack Tip Stress Fields," Mechanics Today, Vol. III (S. Nemat-Nasser, editor), Pergamon, New York, in press.
6. G. C. Sih (editor), Mechanics of Fracture, Methods of Analysis and Solutions of Crack Problems, Noordhoff International Publishing, Leyden, 1973.
7. A. Sommerfeld, Optics, Academic Press, New York, 1954.
8. A. W. Maue, "Die Kantenbedingungen in der Beugungstheorie elastischer Wellen," Z. Naturforschg. 7a, 1952, p. 387.
9. L. B. Freund and R. J. Clifton, "On the Uniqueness of Elastodynamic Solutions for Running Crack," J. Elasticity 4, 1974, p. 293.
10. S. N. Karp and F. C. Karel, Jr., "The Elastic-Field Behavior in the Neighborhood of a Crack of Arbitrary Angle," Com. P. and Appl. Math. XV, 1962, p. 413.
11. J. D. Achenbach and Z. P. Bažant, "Elastodynamic Near-Tip Stress and Displacement Fields for Rapidly Propagating Cracks in Orthotropic Materials," J. Appl. Mech. 42, 1975, p. 183.
12. E. H. Yoffe, "The Moving Griffith Crack," Phil. Mag. 42, 1951, p. 739.
13. B. R. Baker, "Dynamic Stresses Created by a Moving Crack," J. Appl. Mech. 29, 1962, p. 449.
14. A. T. deHoop, Representation Theorems for the Displacement in an Elastic Solid and their Application to Elastodynamic Diffraction Theory, Doctoral Dissertation, Technische Hogeschool, Delft, 1958.
15. S. A. Thau and T. H. Lu, "Transient Stress-Intensity Factor for a Finite Crack in an Elastic Solid Caused by a Dilatational Wave," Int. J. Solids Struct. 7, 1971, p. 731.
16. Z. P. Bažant, J. L. Glazik, Jr., J. D. Achenbach, "Finite Element Analysis of Wave Diffraction by a Crack," J. Eng. Mech. Div., ASCE, 1976 (in press).
17. J. M. Anderson, J. A. Aberson and W. W. King, "Finite Element Analysis of Cracked Structures Subjected to Shock Loads," Computational Fracture Mechanics (L.F. Rybicki, editor), ASME, New York, 1975.
18. Y. M. Chen, "Numerical Computation of Dynamic Stress Intensity Factors by a Lagrangian Finite-Difference Method (The Hemp Code)," Eng. Fracture Mech 7, 1975, p. 653.
19. J. L. Glazik, Jr., Numerical Analysis of Elastodynamic Near-Tip Stress Fields for Stationary and Propagating Cracks, Ph.D. Dissertation, Northwestern University, Evanston, Ill., 1976.
20. L. B. Freund, "The Stress Intensity Factor due to Normal Impact Loading of the Faces of a Crack," Int. J. Engng. Sc. 12, 1974, p. 179.
21. L. B. Freund and J. R. Rice, "On the Determination of Elastodynamic Crack Tip Stress Fields," Int. J. Solids Struct. 10, 1974, p. 411.
22. L. B. Freund, "Crack Propagation in an Elastic Solid Subjected to General Loading, II. Nonuniform Rate of Extension," J. Mech. Phys. Solids 20, 1972, p. 141.
23. B. V. Kostrov, "On the Crack Propagation with Variable Velocity," Int. J. of Fracture 11, 1975, p. 47.
24. K. B. Broberg, "The Propagation of a Brittle Crack," Arkiv F. Fysik 18, 1960, p. 159.
25. A. Kamei and T. Yokobori, "On the Stress Distribution ahead of a Propagating Elastic Brittle Crack," Strength and Fracture of Materials, 3, 1967, p. 103.
26. J. R. Willis, "Self-Similar Problems in Elastodynamics," Phil. Trans. Roy. Soc. London 274, 1973, p. 435.
27. M. L. Williams, "The Stresses around a Fault or Crack in Dissimilar Media," Bul. Seism. Soc. America 49, 1959, p. 199.
28. J. D. Achenbach, Z. P. Bažant and R. P. Khetan, "Elastodynamic Near-Tip Fields for a Rapidly Propagating Interface Crack," Int. J. Engng. Sc., in press.
29. C. Atkinson, "Dynamic Crack Problems in Dissimilar Media," Mechanics of Fracture Vol. IV, Elastodynamic Crack Problems (G. C. Sih, editor), Noordhoff Int. Leyden, in press.

Unclassified

SECURITY CLASSIFICATION OF THIS PAGE (When Data Entered)

REPORT DOCUMENTATION PAGE		READ INSTRUCTIONS BEFORE COMPLETING FORM
1. REPORT NUMBER NU - SML TR No. 76-1 ✓	2. GOVT ACCESSION NO.	3. RECIPIENT'S CATALOG NUMBER
4. TITLE (and Subtitle) Wave Propagation, Elastodynamic Stress Singularities, and Fracture ✓	5. TYPE OF REPORT & PERIOD COVERED Interim	
	6. PERFORMING ORG. REPORT NUMBER	
7. AUTHOR(s) J. D. Achenbach	8. CONTRACT OR GRANT NUMBER(s) N00014-76-C-0063 ✓	
9. PERFORMING ORGANIZATION NAME AND ADDRESS Northwestern University Department of Civil Engineering Evanston, IL 60201	10. PROGRAM ELEMENT, PROJECT, TASK AREA & WORK UNIT NUMBERS ONR-064-483/474	
11. CONTROLLING OFFICE NAME AND ADDRESS Office of Naval Research ✓ Structural Mechanics Program Department of the Navy, Arlington, Va. 22217	12. REPORT DATE May 1976 ✓	
	13. NUMBER OF PAGES 17	
14. MONITORING AGENCY NAME & ADDRESS (if different from Controlling Office)	15. SECURITY CLASS. (of this report) UNCLASSIFIED	
	15a. DECLASSIFICATION/DOWNGRADING SCHEDULE	
16. DISTRIBUTION STATEMENT (of this Report) Approved for public release, distribution unlimited		
17. DISTRIBUTION STATEMENT (of the abstract entered in Block 20, if different from Report)		
18. SUPPLEMENTARY NOTES Presented as a Sectional Lecture at the 14th International Congress of Theoretical and Applied Mechanics, and published in the Proceedings.		
19. KEY WORDS (Continue on reverse side if necessary and identify by block number) fracture elastodynamics stress singularities cracks		
20. ABSTRACT (Continue on reverse side if necessary and identify by block number) The singular part of the elastodynamic field in the vicinity of a crack tip plays an important role in fracture mechanics considerations. In this paper analytical, numerical and experimental methods to determine near-tip elastodynamic fields are reviewed, and the interpretation of stress intensity factors is discussed within the context of the fracture criterion of the balance of rates of energies. We consider elastodynamic effects generated by rapid propagation of the crack as well as by the diffraction of incident stress waves. Propagation in the plane of the crack, as well as skew crack propagation and crack		

DD FORM 1 JAN 73 1473

EDITION OF NOV 65 IS OBSOLETE
S/N 0103-014-6601-1

* are considered.

SECURITY CLASSIFICATION OF THIS PAGE (When Data Entered)

30. H. Kolsky, Stress Waves in Solids, Dover, New York, 1963.
31. H. Kolsky and D. Rader, "Stress Waves and Fracture," Fracture I (H. Liebowitz, editor) Academic Press, New York, 1969, p. 553.
32. F. Kerkhof, Bruchvorgänge in Gläsern, Verlag der Deutschen Glastechnischen Gesellschaft, Frankfurt (Main), 1970.
33. G. C. Sih (editor), Dynamic Crack Propagation, Noordhoff Int. Publishing, Leyden, 1973.
34. M. Stern (editor), Proc. 12th Annual Meeting of the Society of Engineering Science, U. of Texas at Austin, 1975.
35. G. C. Smith and W. G. Knauss, "Experiments on Critical Stress Intensity Factors resulting from Stress Wave Loading," Mech. Res. Comm 2, 1975, p. 187.
36. C. Atkinson, and J. D. Eshelby, "The Flow of Energy into the Tip of a Moving Crack," Int. J. Fract. Mech 4, 1968, p. 3.
37. B. V. Kostrov and L. V. Nikitin, "Some General Problems of Mechanics of Brittle Fracture," Arch. Mech. Stos. 22, 1970, p. 749.
38. L. B. Freund, "Energy Flux into the Tip of an Extending Crack in an Elastic Solid," J. of Elasticity 2, 1972, p. 341.
39. J. W. Miles, "Homogeneous Solutions in Elastic Wave Propagation," Quart. Appl. Math XVIII, 1960, p. 37.
40. V. I. Smirnov, A Course of Higher Mathematics. English translation, Vol. III, Pergamon Press and Addison-Wesley Publ. Co., New York, 1964, p. 203.
41. G. P. Cherepanov and E. F. Afanasev, "Some Dynamical Problems of the Theory of Elasticity," PMM 37, 1973, p. 618 (also Int. J. Eng. Sc. 12, 1974, p. 665).
42. L. Knopoff, "Elastic Wave Propagation in a Wedge," Wave Propagation in Solids (J. Miklowitz, editor) ASME, New York, 1969.
43. B. V. Kostrov, "Diffraction of a Plane Wave by a Smooth Rigid Wedge in an Unbounded Elastic Medium in Absence of Friction," PMM 30, 1966, p. 198 (in translation P. 244).
44. J. D. Achenbach, "Shear Waves in an Elastic Wedge," Int. J. Solids Struct. 6, 1970, p. 379.
45. J. D. Achenbach and V. K. Varatharajulu, "Skew Crack Propagation at the Diffraction of a Transient Stress Wave," Quart. Appl. Math XXXII, 1974, p. 123.
46. J. D. Achenbach, "Bifurcation of a Running Crack in Anti-plane Strain," Int. J. Solids Struct. 11, 1975, p. 1301.
47. J. D. Achenbach, "Skew Crack Propagation under Stress-Wave Loading," Mech. Res. Comm. 1, 1974, p. 325.
48. J. Congleton, "Practical Applications of Crack-Branching Measurements," Dynamic Crack Propagation (G. C. Sih, editor), Noordhoff, Leyden, 1974, p. 427.
49. A. B. J. Clark and G. R. Irwin, "Crack Propagation Behaviors," Experimental Mechanics, 6, 1966, p. 321.
50. A. S. Kobayashi, B. G. Wade, W. B. Bradley and S. T. Chiu, "Crack Branching in Homalite-100 sheets," Engng. Fract. Mech. 6, 1974, p. 81.
51. W. Döll, "Investigations of the Crack Branching Energy," Int. J. Fract. Mech 11, 1975, p. 184.

ACCESSION for	
NTIS	White Section <input checked="" type="checkbox"/>
DOC	Buff Section <input type="checkbox"/>
UNANNOUNCED	<input type="checkbox"/>
JUSTIFICATION	
BY	
DISTRIBUTION/AVAILABILITY CODES	
Dist.	AVAIL. # of copies
A	